AFGL-TR-77-0179

ACCELEROMETER SYSTEM FOR

S77-2 SATELLITE

William G. Lange

Bell Aerospace Textron
P. O. Box One
Buffalo, New York 14240

FINAL REPORT

Period Covered: 24 March 1976 through 30 June 1977

30 June 1977

Approved for public release; distribution unlimited

Prepared
for

AIR FORCE GEOPHYSICS LABORATORY
AIR FORCE SYSTEMS COMMAND
UNITED STATES AIR FORCE
HANSCOM AFB, MASSACHUSETTS 01731

Unclassified

SECURITY CLASSIFICATION OF THIS PAGE (When Data Entered)

REPORT DOCUMENTATION PAGE		READ INSTRUCTIONS BEFORE COMPLETING FORM
1. REPORT NUMBER (18) (19) AFGL-TR-77-0179	2. GOVT ACCESSION NO.	3. RECIPIENT'S CATALOG NUMBER (9) Final rept. 24 Mar 76-30
4. TITLE (and Subtitle) (6) ACCELEROMETER SYSTEM FOR S77-2 SATELLITE,		5. TYPE OF REPORT & PERIOD COVERED Final - 24 March 1976 to 30 June 1977
		6. PERFORMING ORG. REPORT NUMBER (14) 6350-923016
7. AUTHOR(s) (10) William G./Lange		8. CONTRACT OR GRANT NUMBER(s) (15) F19628-76-C-0120 New
9. PERFORMING ORGANIZATION NAME AND ADDRESS Bell Aerospace Textron P. O. Box One Buffalo, New York 14240		10. PROGRAM ELEMENT, PROJECT, TASK AREA & WORK UNIT NUMBERS 62101F (16) 66900202 (17) 02
11. CONTROLLING OFFICE NAME AND ADDRESS Air Force Geophysics Laboratory Hanscom AFB, Massachusetts 01731 Contract Monitor: Frank A. Marcos/LKB		12. REPORT DATE (11) 30 Jun[redacted]77
		13. NUMBER OF PAGES 26 (12) 26p.
14. MONITORING AGENCY NAME & ADDRESS (if different from Controlling Office)		15. SECURITY CLASS. (of this report) Unclassified
		15a. DECLASSIFICATION/DOWNGRADING SCHEDULE

16. DISTRIBUTION STATEMENT (of this Report)

Approved for public release; distribution unlimited.

17. DISTRIBUTION STATEMENT (of the abstract entered in Block 20, if different from Report)

18. SUPPLEMENTARY NOTES

408 855

19. KEY WORDS (Continue on reverse side if necessary and identify by block number)

Accelerometer	Aerodynamic Drag
Acceleration	Air Density
Drag	Electrostatic Accelerometer

20. ABSTRACT (Continue on reverse side if necessary and identify by block number)

cont'd p1

This report describes development, fabrication and test of an accelerometer system for use in the S77-2 Satellite, and covers the period 24 March 1976 through 30 June 1977.

One accelerometer system and one set of Ground Support Equipment were delivered to AFGL in the course of this contract.

DD FORM 1 JAN 73 1473 EDITION OF 1 NOV 65 IS OBSOLETE

Unclassified

SECURITY CLASSIFICATION OF THIS PAGE (When Data Entered)

I. INTRODUCTION

This report describes the design, and development, fabrication and test of an analog voltage constrained electrostatic accelerometer to measure upper atmospheric density in an Air Force satellite designated S77-2. (cont on p 1473A)

II. SYSTEM APPROACH

The contractual engineering specification required acceleration measurements over the range of 10^{-3} to 10^{-8}g with an accuracy of 0.2% or better while operating in a spacecraft temperature environment of 25^{o}F to 110^{o}F for a period of six months.

A system was designed to meet these requirements using the approach described herein.

The sensitive axis could be commanded to measure two different full-scale input levels. These were designated range A and B as follows:

$$A = 8 \times 10^{-3} g$$

$$B = 4 \times 10^{-4} g$$

The cross axis or suspension scaling could also be commanded into one of two ranges to reduce the magnitude of tne null bias. These were also designated range A and B as follows:

$$A = 1 \quad g$$

$$B = 10^{-3} g$$

The A scale is automatically in effect for the first 25 seconds after power is applied to provide the force required to initially suspend the proof mass.

The temperature of each instrument is telemetered and appears as a 0 to +5 V dc signal. It will be used to correct the scale factor for temperature effects.

The acceleration output signal is made available at the experiment/spacecraft in serial form on two 8 bit words. These words are sampled once every 1/4 second as two adjacent words on the telemetry main frame.

The error budget shown below has been established for the three major sections of the system to meet the 0.2% accuracy requirement. The budget is based on experience with previous systems plus test data from the development model.

Instrument and Instrument Electronics	.15%
Pulse Rate Converter	.022%
Counter	.006%
	.178%

A more detailed description of the instrument and theory of operation is contained in Section VI.

III. MECHANICAL DESIGN

The structural foundation of the system is an aluminum machined base plate. Mounted to the plate are the accelerometer and system electronics. The accelerometer assembly is enclosed (non-hermetically) by a drawn aluminum cover resulting in a rectangular package 3.6 inches high, 4.4 inches wide, and 9 inches long.

The accelerometer assembly is mounted on a rotating base which indexes the sensitive axis in one of two positions. The position may be changed by ground command. The base/satellite mechanical interface is a 6 inch square aluminum plate with four corner mounting holes. The complete assembly with the accelerometer mounted on the base has maximum dimensions of 6.4 inches high and a 9.0 inch length and width. The total weight is 11.1 pounds.

Thermal analysis of the system indicates a maximum internal temperature of 65°C occurring when the environmental (spacecraft) temperature is at 50°C and when the system is operating at its maximum power rating of 6.5 watts. Combined heat transfer modes of conduction and radiation were assumed. Radiating surfaces were assigned an emissivity of 0.9, corresponding to black anodized aluminum.

The accelerometer consists of several precision mechanical components mounted in a hermetically sealed, electron beam welded, hexogon shaped housing. Six printed circuit boards carrying sensor electronics are mounted to the flats on the housing and are interfaced with each other and the system electronics via an interconnect board located at the top of the instrument. Ten (10) hermetic feed-through terminals mounted on three of the flats carry electrical functions (forcing, constrainment, and pick-off) between instrument internal electrodes and the sensor electronics.

IV. ELECTRICAL DESIGN

A. Instrument Electronics

The instrument electronics constrains the proofmass in both the sensitive and cross axis. The constrainment loop parameters are determined by two range relays which can be overridden by an over-range command whenever the input exceeds the full scale limits of the lower range.

It also generates normalized analog output signals proportional to the acceleration input. This output is fed to a Voltage to Frequency converter (PRC).

B. System Electronics

Primary unregulated power from the spacecraft enters the connector on separate power and return lines. A common chassis ground pin is provided. Power then passes through three stages of conditioning for use by the various circuits.

The EMI filter section has provisions for transient attenuation and bi-directional suppression of conducted electromagnetic interference. This is followed by a voltage regulator which isolates the system from the 24V to 32V line variation. The DC-DC converter establishes the working voltage levels for the system's electronics.

The DC-DC converter design is based on a saturable core transformer with the primary switching transistors driven regeneratively by two of its windings. The transformer secondary is tapped

to provide the five operating voltage levels for the system's electronics. Rectification and filtering follow to provide dc outputs at +45v, -45v, +15v, -15v and +5v for a primary input voltage of +21v ± .01% frcm the voltage regulator. Secondary load regulation is ±2%.

The voltage to frequency (pulse rate converter) performs analog to digital conversion on the current received from the constrainment subsystem. The pulse rate converter uses the pulse-constrained integrator principal and consists of an integrator, a precision charge pulse generator, and a trigger/logic system. A block diagram is shown below.

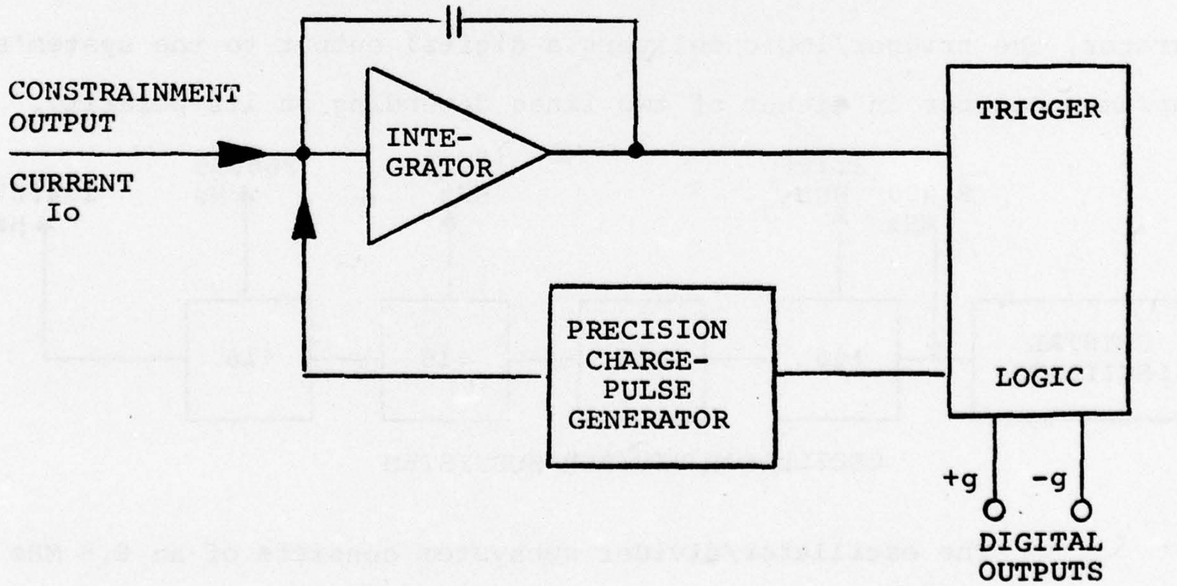

Assume a positive input current, Io, is applied to the integrator. The integrator output, Eo, in response to this input, moves from 0 volt level to an output trigger level, $-Eo_1$. When Eo

reaches $-Eo_1$, the trigger/logic circuit commands the pulse generator to deliver a negative pulse. A dc pulse of fixed charge, Qp, is generated by the pulse generator and summed into the integrator. This pulse, which is opposite in polarity to Io, causes the integrator output to return toward the 0 volt level.

The integrator output again moves toward $-Eo_1$, whereupon, the cycle is repeated. For the integrator to remain constrained, the average current flow into the summing point must be zero. Hence,

$$Io = fQp$$

where: Io = the input current

Qp = the constraining pulse charge

f = pulse repetition rate

Thus, the pulse rate is directly proportional to the input current.

When a constraining pulse is being summed into the integrator, the trigger/logic delivers a digital output to the system's up/down counter on either of two lines depending on its polarity.

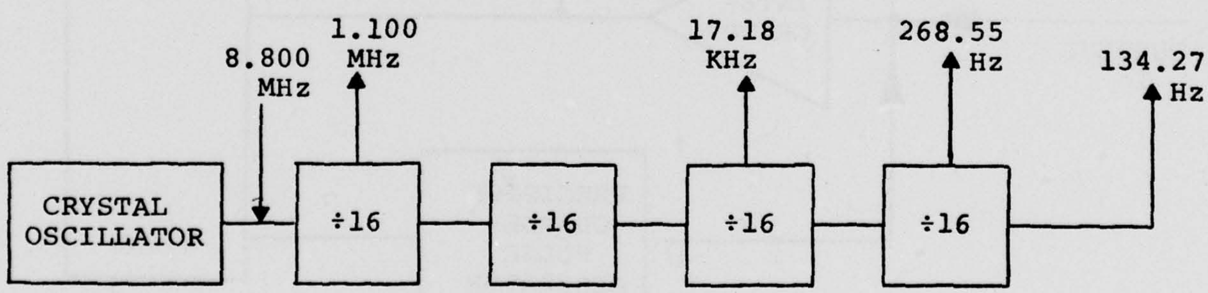

OSCILLATOR/DIVIDER SUBSYSTEM

The oscillator/divider subsystem consists of an 8.8 MHz crystal oscillator and four cascades 4-bit binary counters. It provides the frequency references used by the various subsystems.

The crystal frequency was chosen to provide a 1.1 MHz signal for the suspension system. The remaining frequencies are used in the constrainment and overrange timing circuits.

The digital signal conditioner (counter) subsystem receives pulse rate and polarity data internally from the pulse rate converter. It receives the gate pulse and data clock signals from the spacecraft and outputs test pulses and two 8-bit serial data words to the spacecraft through the output connector.

The digital signal conditioner consists of a pulse interlock circuit, an up/down counter, a shift register, and a counter control circuit. During normal operation, pulses from the PRC pass directly through the pulse interlock circuit and are stored in the up/down counter. Upon receipt of a word enable command, the counter control enables the pulse interlock circuit.

The data in the up/down counter, along with the system overrange information, is strobed into the shift register and the counter is reset. If a pulse occurs during this interval of approximately 30 μsec, it is stored in the pulse interlock circuit and then passed on at the interval's end. The counter control then toggles the shift register in synchronism with the PCM shift clock providing a serial output.

C. <u>Rotating Base Electronics</u>

Base rotation is accomplished with a reversing d-c motor and gear train. Upon receipt of a position command, 28 volt power is applied to the motor to cause it to rotate the base until it reaches its

new position 90° from the previous position. Limit switches interrupt the power after the base has been driven against a spring loaded mechanical stop.

Subsequent receipt of another position command energizes a relay which reverses the 28 volt power polarity and causes the motor to rotate the base in the opposite direction, back to its original position.

A single 0 to 5 V TM line is used to monitor the base position at all times. This line assumes 3 discrete voltage levels as follows:

Position X	3.9 volts
Position Y	2.2 volts
Rotating between stops	0.8 volts

V. TEST REQUIREMENTS

Figure 1 indicates the phases and sequence of testing from incoming parts to delivery.

A. Incoming Parts

Parts testing and screening by Bell Aerospace Textron is not performed on items procured under numbers (1) and (2). Parts procured under (3) and (4) are 100% functionally tested. In the case of hybrid microcircuits, screening tests are performed either by Bell Aerospace Textron or the supplier. These screening tests include as a minimum, precap inspection, thermal shock, leak tests and burn-in.

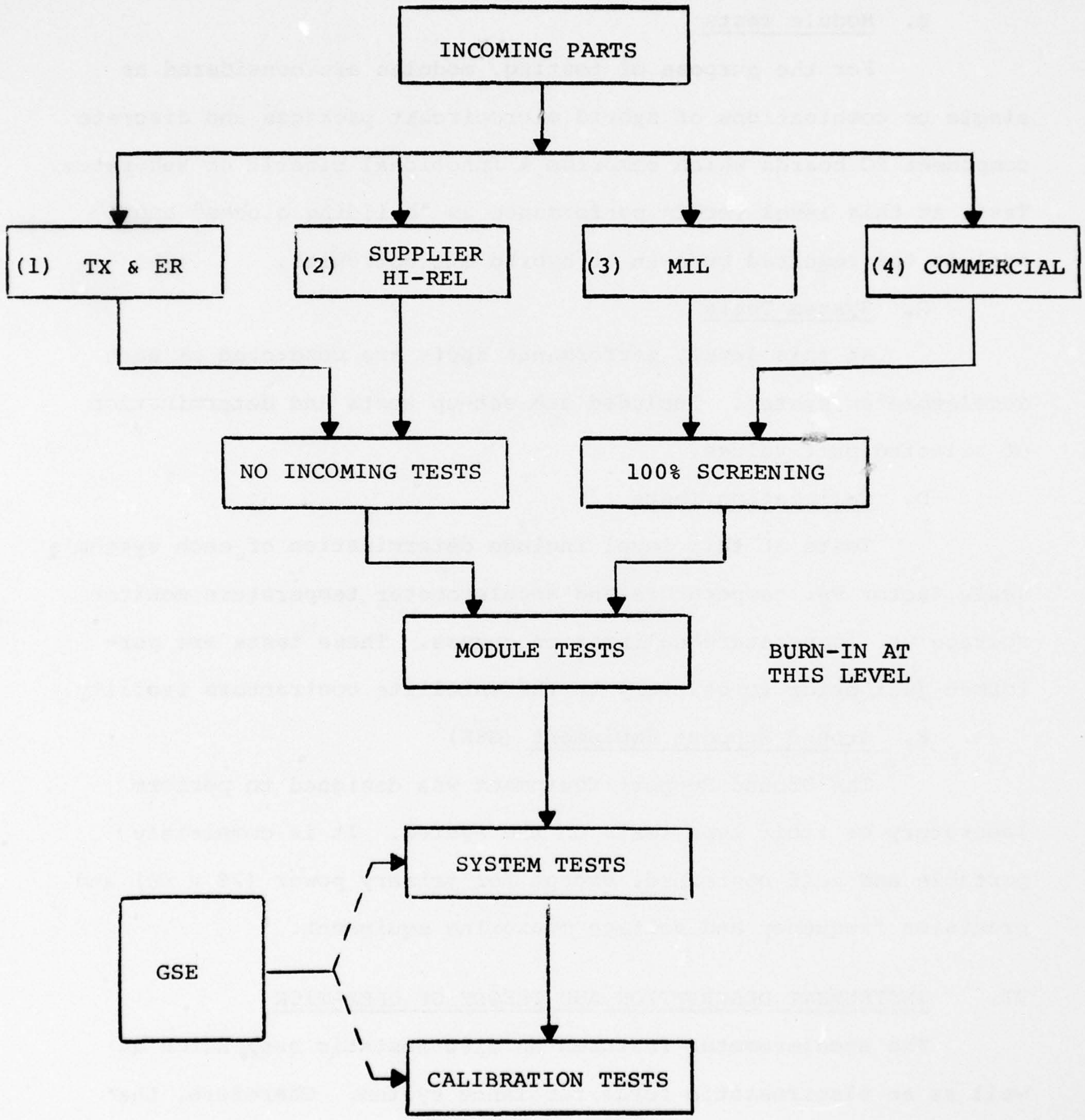

FIGURE 1. <u>PARTS TO SYSTEM TEST SEQUENCE</u>

B. <u>Module Tests</u>

For the purpose of testing, modules are considered as single or combinations of hybrid microcircuit packages and discrete component PC boards which comprise a functional circuit or subsystem. Tests at this level verify performance as "building blocks" and include the required burn-in of hybrid microcircuits.

C. <u>System Tests</u>

At this level, performance tests are conducted on each accelerometer system. Included are set-up tests and determination of selected part values.

D. <u>Calibration Tests</u>

Tests at this level include determination of each system's scale factor vs. temperature and accelerometer temperature monitor voltage vs. temperature calibration curves. These tests are performed just prior to delivery to the satellite contractors facility.

E. <u>Ground Support Equipment</u> (GSE)

The Ground Support Equipment was designed to perform laboratory or field type tests on the system. It is completely portable and self contained, except for primary power (28 v dc) and precision frequency and voltage measuring equipment.

VI. INSTRUMENT DESCRIPTION AND THEORY OF OPERATION

The accelerometer features an electrostatic suspension as well as an electrostatic force rebalance system. Therefore, the scaling of both the suspension system and the force rebalance system can be changed at will by simply changing voltage levels.

The proofmass consists of a beryllium cylinder with a flange. The sensitive axis is parallel to the longitudinal axis of the cylinder and the suspension axis is normal to the cylinder walls. The electrode carrier has eight, metal-coated areas and slips inside the proofmass cylinder. These metallized areas constitute the primary elements of the suspension system. The two forcer blocks slip over the proofmass cylinder and are separated from each other by a spacer ring so that the proofmass has a small freedom of motion along the cylinder (sensitive) axis (Figure 2).

Each forcer block has three annular rings. The inner and outer rings are of equal area and constitute the forcer electrodes. The middle rings are the capacitive pickoffs which sense motion.

Acceleration along the sensitive axis causes the proofmass to be displaced slightly from its null or zero acceleration position. This displacement causes the force rebalance system to change the voltages on the forcer electrodes thereby generating the electrostatic force required to exactly balance the acceleration force.

Acceleration Measurements

Conventionally, high-precision acceleration measurements are made by determining the force required to constrain a proofmass against an unknown input acceleration applied to its case. Instruments of this type are called force rebalance accelerometers and are an application of Newton's second law of motion:

$$F = Ma$$

Figure 2

where:

M = mass of the proofmass

a = acceleration

F = Force required to accelerate the proofmass

Force rebalance can be accomplished by a number of methods. Typical examples are a spring, a string under tension, or a force applied by a feedback technique which continuously nulls the deflection of the proofmass with respect to its case through a high-gain feedback amplifier. The force can be generated electromagnetically, electrostatically or some other way.

Since conventional force rebalance accelerometers are electromechanical devices, their scaling and environmental capabilities are determined and fixed when they are designed and fabricated. For example, an accelerometer designed for a 50g environment has to have a cross axis suspension system of proofmass and force rebalance capability of at least that magnitude, and probably two or three times greater. As a rule, the cross coupling of the suspension forces in the sensitive axis is in the ratio of about 10^{-5} to 10^{-6}. It can, therefore, be expected that a proofmass suspended in the cross axis for 100g capability introduces a null error of approximately 10^{-4}g along the sensitive axis.

One method of achieving a low-g accelerometer would be to disassemble the instrument in the essentially zero-g environment of space and substitute a fine hair for the relatively stiff suspension spring of the proofmass. This, of course, is not practical since it would require an instrument laboratory and calibration test facility. A practical way of achieving the same effect is inherent in the MESA instrument design.

Suspension Subsystem

The purpose of the suspension subsystem is to support the proofmass cylinder radially to permit free movement in the axial direction. Furthermore, the suspension forces have to be adjustable for the particular environment; at least 1g on the earth and in the order of 10^{-2}g or less in space. Since it is not possible to fabricate a perfect cylinder, it is necessary to reduce the suspension force to prevent cross coupling of the suspension force into the sensitive axis.

The electrostatic force, due to a potential difference, is given by the equation:

$$F = 4.4 \times 10^{-7} \frac{K V^2 A}{\delta^2} \qquad (1)$$

where: F = resultant force (dynes)

K = dielectric constant

V = potential difference (volts)

A = area of electrode (sq. cm)

δ = gap between the electrodes and the proofmass (cm)

Differentiating this equation with respect to a small change in the gap, yields:

$$\Delta F = 2F_o \frac{\Delta\delta}{\delta_o} \qquad (2)$$

where: ΔF = the change in force

$\Delta\delta$ = the small change in gap

F_o = nominal suspension force exerted on the proofmass

δ_o = nominal gap between proofmass and electrodes

This equation shows that the rate of force decrease is twice the rate of gap increase and that the proofmass will always "touch down" under the influence of any cross-axis acceleration.

To keep the proofmass suspended, the voltage of a particular electrode has to be adjusted to overcome the basic suspension instability, as a result of change in gap, expressed in equation (2). This could be accomplished by an active system which measures the radial deflection of the proofmass and, through a high-gain feedback loop, generates electrode voltages to keep the proofmass suspended.

To circumvent the complexity of an active suspension system requiring a pickoff and feedback amplifier, a tuning technique has been developed which utilizes the capacitance between the electrodes and the proofmass. This capacitance increases as the proofmass approaches the electrode carrier and decreases as it moves away. This relatively simple suspension technique is illustrated in Figures 3 and 4.

The relationships between the electrode voltages V_{E1} and V_{E2}, as a function of frequency and suspension load, are shown in Figure 4 for the condition of no cross axis acceleration and for a 1g condition. The frequency of the suspension voltage (E_s) has been selected slightly above the resonant frequency.

Under the no-load suspension condition, the electrode voltages V_{E1} and V_{E2} are approximately equal because gaps δ_1 and δ_2 and, therefore, capacitances C_1 and C_2 are equal. When a cross-axis

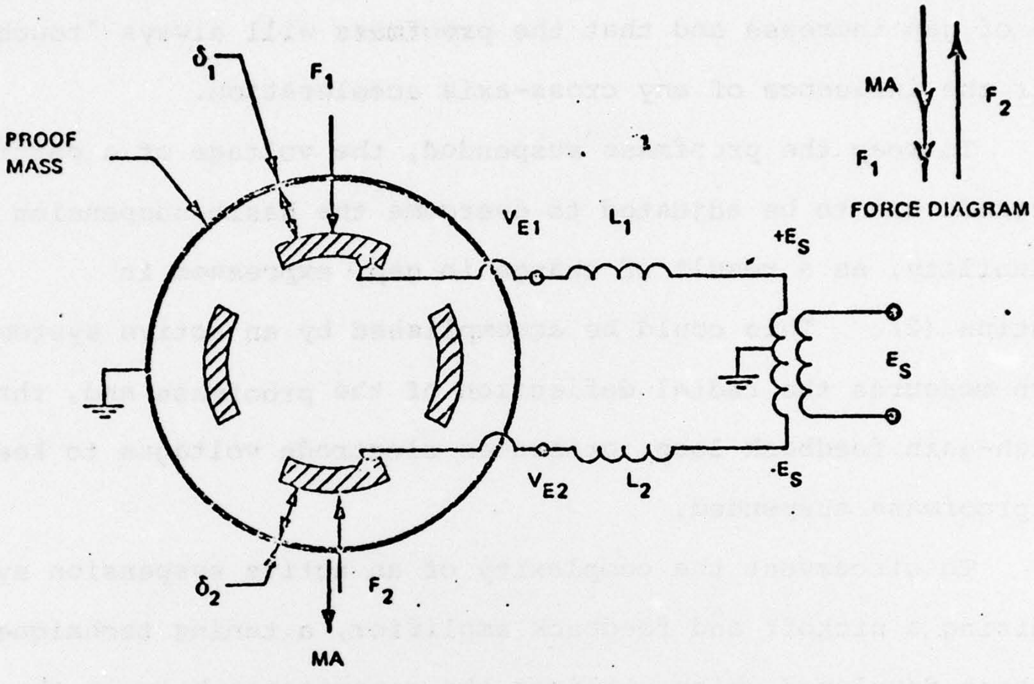

Figure 3 Schematic and Force Diagram of MESA

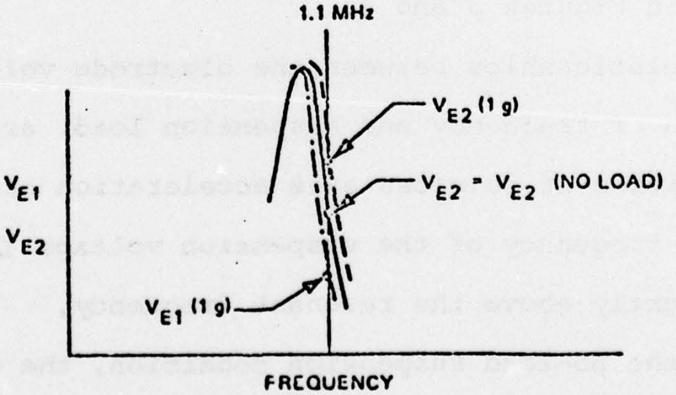

Figure 4. Electrode Voltages V_{E1} and V_{E2} as a Function of Frequency for No Load and 1g Suspension

acceleration is applied, gap δ_1 becomes smaller and capacitance C_1 increases. Since the circuit has a high Q, V_{E1} decreases and its resonant curve shifts to the left. This is indicated by the dash-dotted line. In a similar manner, V_{E2} increases as a result of a decrease of capacitance C_2 and its resonant curve shifts to the right (dashed line). Direction of the restoring force is now such that it will always oppose any radial deflection of the proofmass.

The expression for proofmass radial displacement as a function of cross axis acceleration can be approximated by equation (3).

$$\frac{\Delta\delta}{\delta_o} = \frac{M\ a\ \delta_o^{\ 2}}{4\ (4.4 \times 10^{-7})\ A\ Q_o^{\ 3}\ E_s^{\ 2}} \tag{3}$$

where: $\Delta\delta$ = radial deflection

Q_o = Q of the resonant circuit

E_s = suspension voltage

The other terms have been defined previously.

The initial suspension of the proofmass is achieved by sweeping the suspension voltage frequency from 1.4 MHz to 1.1 MHz. The phase inversion of the suspension voltages on opposing electrodes as shown in Figure 3 keeps the proofmass at ground potential.

Force Rebalance System

When the proofmass is suspended, it is free to move along the cylinder axis (sensitive axis) within the gap set by the spacer ring. An acceleration of the case will cause the proofmass to experience a force which will cause it to move, relative to the case, in a direction opposite to that of the case. This motion is detected by

a capacitance bridge arrangement as shown in Figure 5. The capacitances between the flange of the proofmass and the pickoff rings of the two forcer blocks are inversely proportional to the distances between them. As the proofmass travels toward one forcer block and away from the other, one pickoff capacitance will increase and the other will decrease. For small movements (x) with respect to the normal gaps $_p$, this relationship is linear and the pickoff voltage can be approximated by equation (4):

$$E_o = \frac{2\, K_p\, C\, C_o \frac{x}{\delta p}}{(C + C_o)^2}\; E_c \angle 0^\circ \qquad (4)$$

where:
E_c = excitation voltage to the bridge
E_p = differential amplifier voltage gain
C = fixed capacitors of the bridge
C_o = capacitance between pickoff rings and flange, in centered position
x = deflection of proofmass
δp = gap between flange and pickoff rings, centered position

This capacitance pickoff arrangement has been used in a number of instruments and no threshold has been detected, even into sub-atomic regions.

Figure 6 shows the force rebalance system of the MESA. The pickoff signal is amplified and demodulated to obtain $+V_o$ and $-V_o$ signals which have equal magnitudes but opposite polarity. The magnitudes of $+V_o$ and $-V_o$ are proportional to proofmass displacement

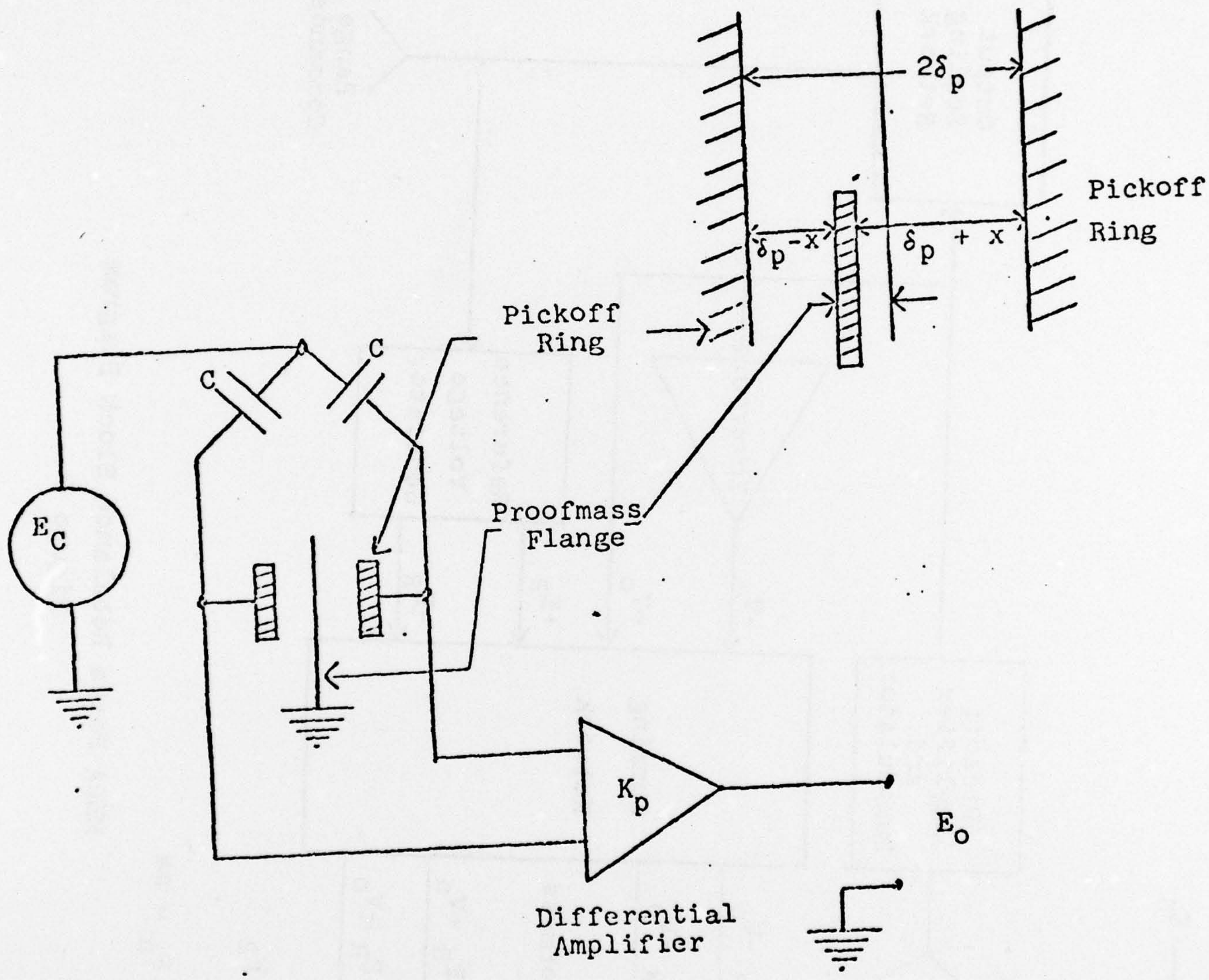

Figure 5. MESA Pickoff System

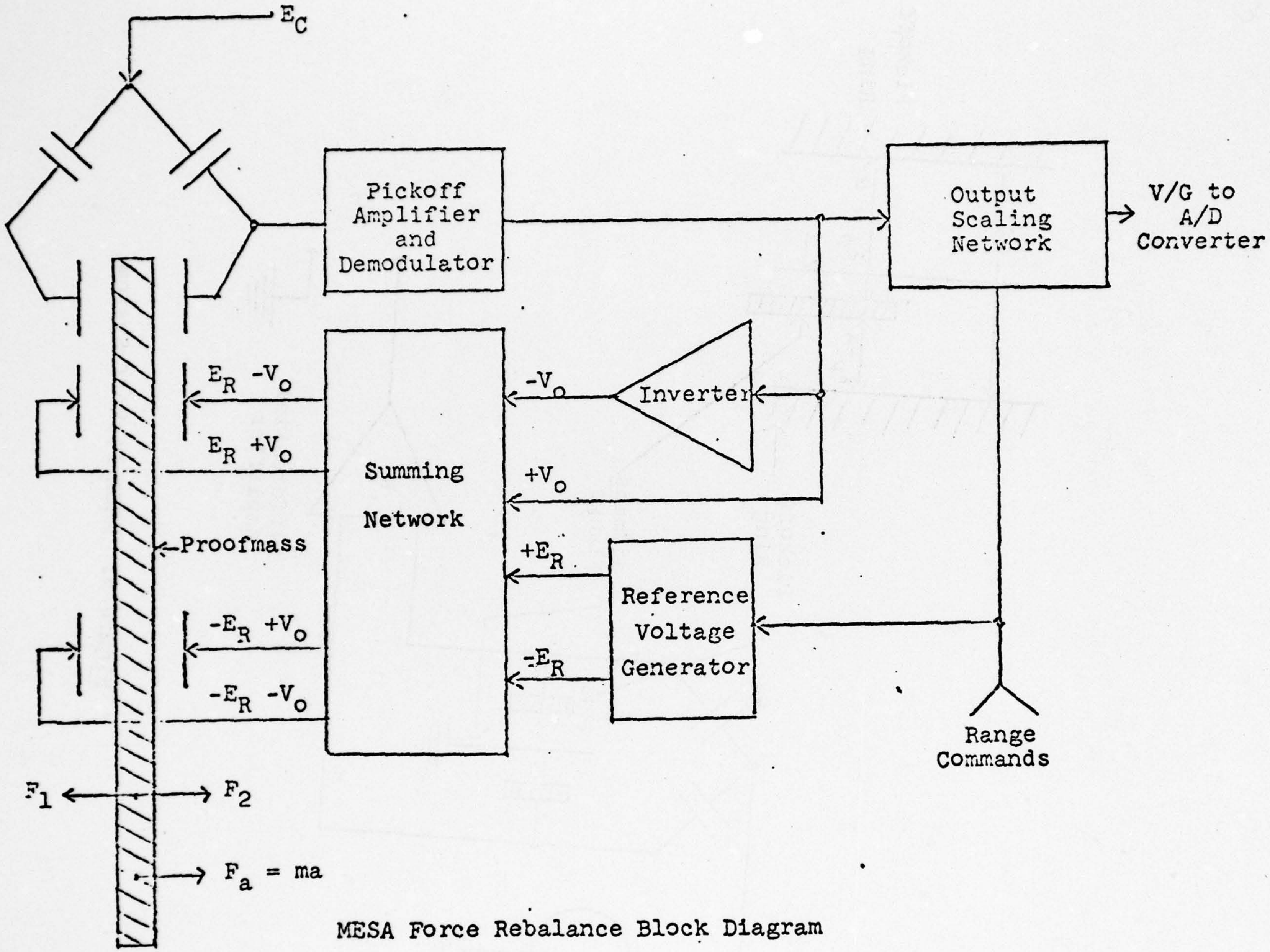

MESA Force Rebalance Block Diagram

Figure 6

and are combined with equal magnitude, opposite polarity reference voltage $+E_R$ and $-E_R$ in a resistive summing network, and applied to the four forcer electrodes.

The force F_a on the proofmass due to input acceleration, a, is balanced by the difference between two electrostatically generated rebalance forces F_1 and F_2, where:

$$F_1 = \frac{4.4 \times 10^{-7} \ KA}{F^2} \left[(E_R + F_o)^2 + (-E_R - V_o)^2 \right]$$

$$F_2 = \frac{4.4 \times 10^{-7} \ KA}{F^2} \left[(E_R - V_o)^2 + (-E_R + V_o)^2 \right]$$

$$F_1 - F_2 = F_a = ma = \frac{4.4 \times 10^{-7} \ KA \ (8 \ E_R)}{\delta_F^{\ 2}} V_o$$

where $\delta_F = \delta_p$ = gap between flange and forcer rings, centered position.

Range scaling of the force rebalance system is achieved by changing the reference voltages $+E_R$ and $-E_R$ in response to constrainment system range commands. These commands also scale the V_o signal to obtain the same full scale analog output voltage on all ranges.

System Configuration

The final system electrical block diagram is shown in Figure 7.

The accelerometer output signal is a d-c voltage proportional to input acceleration. This signal is fed to a precision A/D converter, the output of which is a pulse rate proportional to input

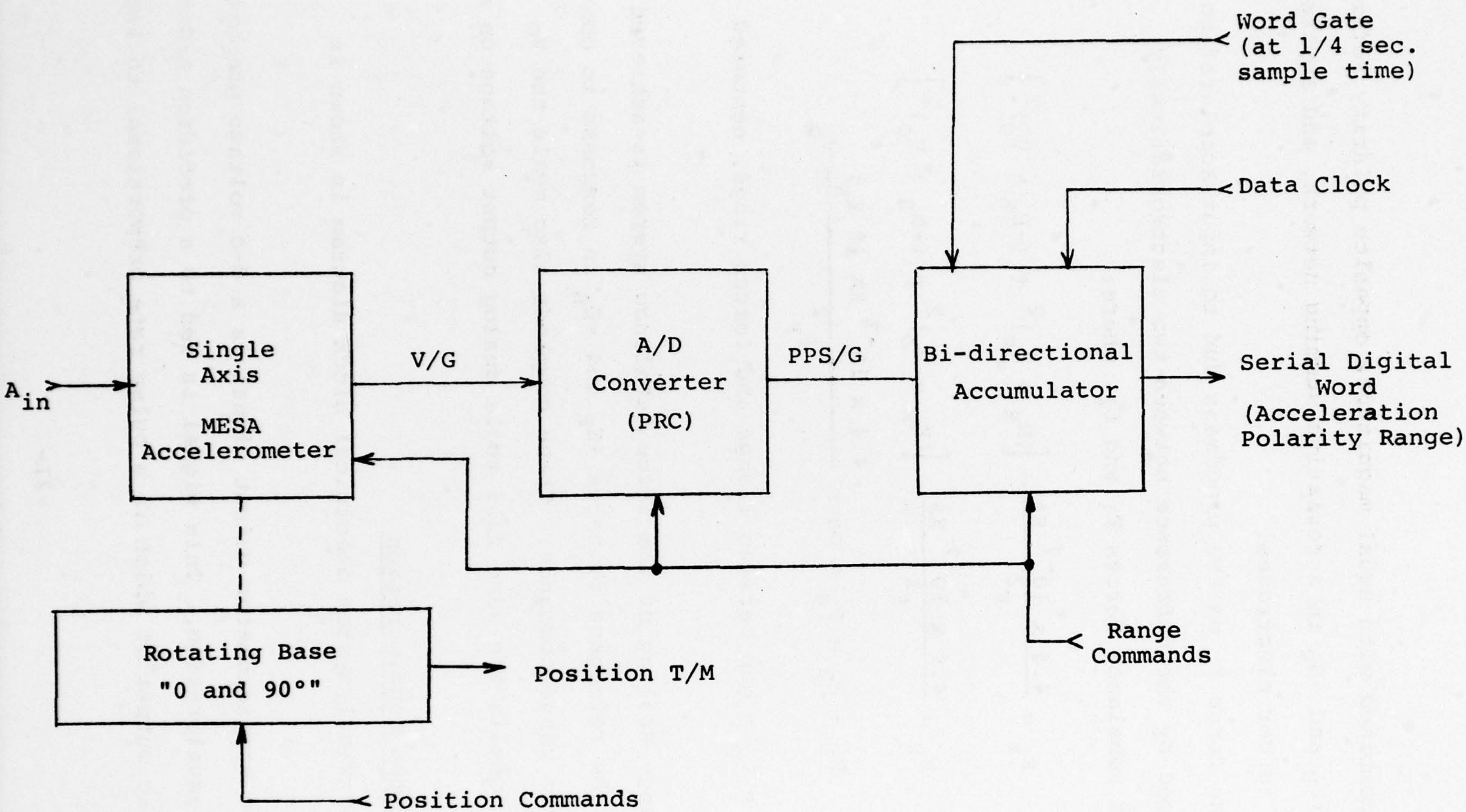

System Electrical Block Diagram

Figure 7

voltage. The pulse rate is now fed to a bi-directional accumulator which counts the number of pulses per sample period and their polarity. At receipt of the word gate, it generates a serial output word which contains the average acceleration experienced over the sample period, the polarity of the acceleration, and the range in effect during that period.

The position of the sensitive axis may be changed by command. The position is monitored by a three level signal which indicates that it is in X, Y, or rotating between the two positions.

Range commands are fed to the constrainment loops within the instrument, the A/D converter, and the bi-directional accumulator.

The mechanical configuration of the accelerometer mounted on the rotating base is shown in Figure 8. The base is fastened to the host vehicle structure by four corner mounting bolts. The power/command and signal interface connectors are mounted directly on the base.

VII. SUMMARY

The design fabrication and test of a single axis accelerometer mounted on a rotating base was accomplished within the scheduled time and will meet the primary objectives of the S77-2 satellite requirements.

Electrical, mechanical, and thermal design interface with the host vehicle contractor were defined. These definitions were finalized in the generation of an Interface Control Document (ICD). System Integration and Environmental tests were conducted to verify the compatibility of the accelerometer and the S77-2 experiment pallet.

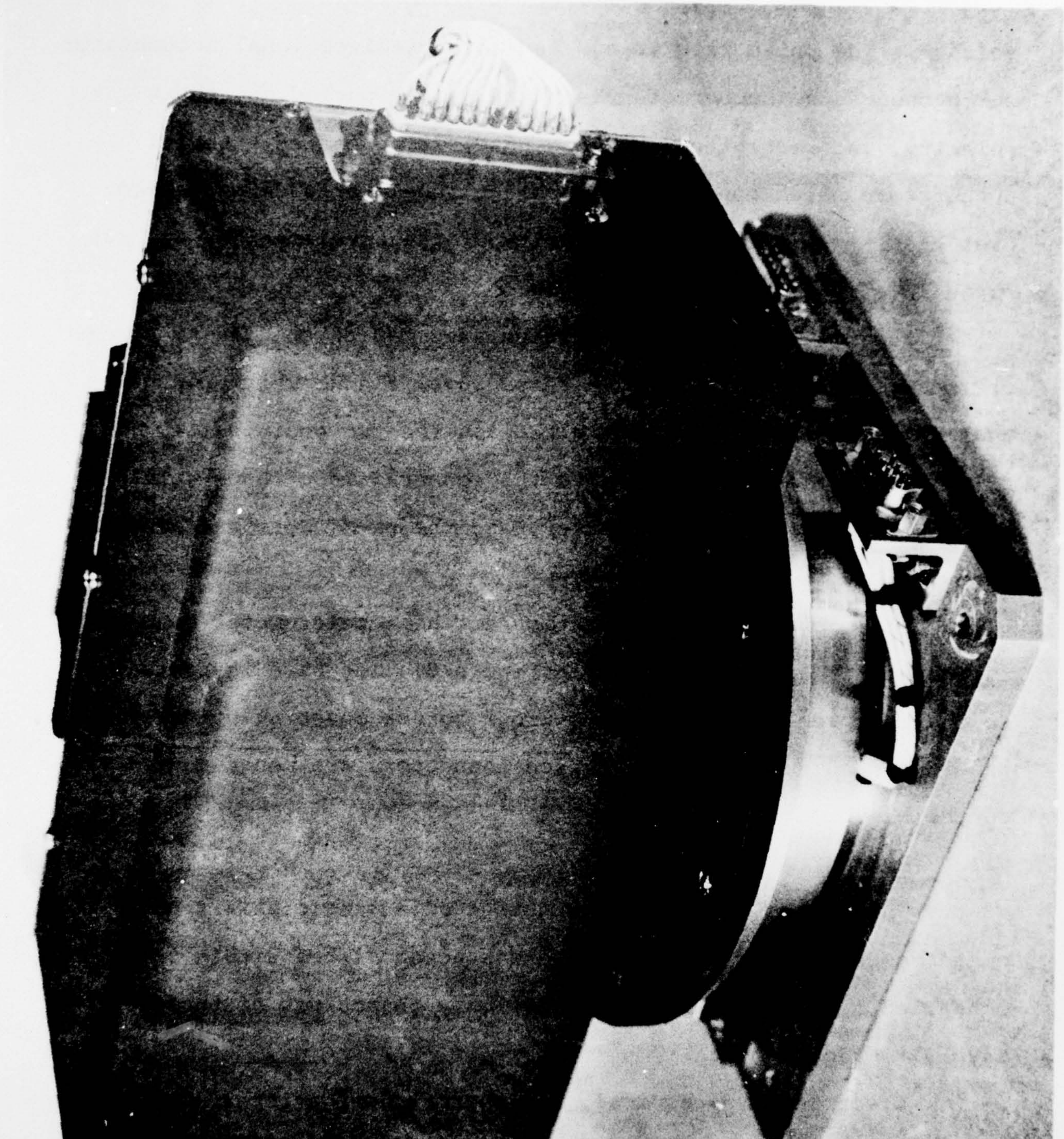

Figure 8. Accelerometer Mounted on Rotating Base